# Fe II complexes supported by an iminophosphorane ligand: synthesis and reactivity

Thibault Tannoux, Louis Mazaud, Thibault Cheisson, Nicolas Casaretto, Audrey Auffrant

# $Fe^{II}$ complexes supported by an Iminophosphorane ligand: Synthesis and Reactivity

Thibault Tannoux,[a] Louis Mazaud,[a] Thibault Cheisson,[a] Nicolas Casaretto,[a] Audrey Auffrant[a]*

The synthesis of iron complexes supported by a mixed phosphine-lutidine-iminophosphorane (PPyNP) ligand was carried out. While a bidentate $\kappa^2$-N,N coordination was observed on $FeCl_2$, pincer coordination modes were adopted at cationic iron centers, either through dechlorination of [LFe(PPyNP)$Cl_2$] (**1**) or direct coordination of PPyNP to $Fe(OTf)_2$. Reaction with tertbutylisocyanide gave access to the diamagnetic octahedral complex [Fe(PPyNP)$(CNtBu)_3]X_2$ (X = OTf (**4**), Cl (**4'**)). Both **1** and **4** were shown to undergo deprotonation of the phosphinomethyl group, but the resulting complexes were not active for the dehydrogenative coupling of hexan-1-ol. Alternatively, the hydrosilylation of acetophenones was catalyzed at room temperature with 1 mol % of a catalyst generated *in situ* from cationic PPyNP supported iron triflate complexes and $KHBEt_3$.

## Introduction

Nitrogen containing ligands are widely used in areas such as coordination and (bio)inorganic chemistry, catalysis, and material sciences.[1, 2] Their nitrogen atoms are generally either $sp^3$ (amine, amide), $sp^2$ (imine and N-heterocycles), or sp (cyanide) hybridized, and they display large structural diversity. For example, various heme[3-6] or non-heme[7-10] N-based ligands were used to develop enzyme mimics. Iminophosphoranes, also named phosphinimines, represent a discrete class of N-ligands where the electron rich nitrogen donor is stabilized by a vicinal phosphonium group. They present a highly polarized P=N bond that can be viewed as a resonance between two limit forms, the neutral ylene and the zwitterionic ylide (Figure 1). Consequently, they behave in coordination chemistry as strong $\sigma$- and $\pi$-donors but show no accepting ability because of the absence of a $\pi$-system.

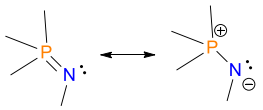

Figure 1: Resonance forms of the iminophosphorane

Iminophosphoranes have been much less investigated than other N-based ligands in coordination chemistry and catalysis.[11-13] Their reported catalytic applications mainly concern polymerization reactions, often with rare earth metals,[14-16] coupling reactions in general with group 10 elements,[17-22] and (transfer)hydrogenations mainly with rhodium(I) and ruthenium(II).[23-30] Examples of iminophosphorane catalysts involving base metal complexes remain limited and this is especially true in the iron case, despite a spectacular development of its coordination chemistry over the past few years,[31-33] that reflects its abundance, low cost, and low toxicity.[34, 35] However, coordination of Fe by bidentate (C,N),[36] (N,N),[37, 38] as well as tridentate (N,C,N) [39-41] and (N,N,N)[42-44] iminophosphorane ligands have been reported.

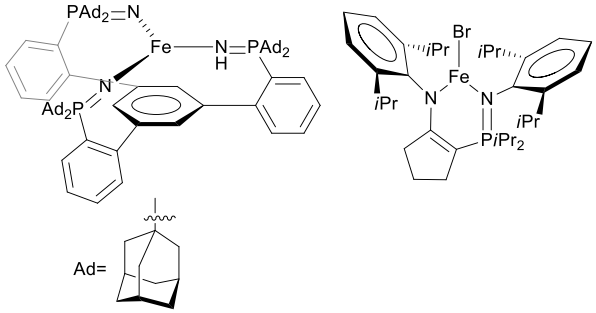


Figure 2: $Fe^{II}$ iminophosphorane complexes for small molecules activation

Low valent iron iminophosphorane complexes have been employed in small molecule activation: Rittle and coworkers recently used a rigid bis(iminophosphorane)imidophosphorane ligand to stabilize a low valent iron(II) prone to activate $O_2$[45] while Fryzuk's group[46] designed an electron rich bidentate iminophosphorane ligand to study iron mediated $N_2$ activation, (Figure 2). Such $N_2$ activation process or N-transfer reactions provided an indirect route to iron complexes featuring an iminophosphorane polydentate ligand from polyphosphine supported complexes.[47-51] Late functionalization via a Staudinger reaction within the coordination sphere of iron has also been reported.[52] Nevertheless, only few iminophosphorane iron complexes have been reported as catalysts (Figure 3). However, about 20 years ago, different groups showed that (N,N,N) and (N,N) Fe complexes have low catalytic ability in ethylene dimerization or polymerization.[42-44] Later iron(II) complexes supported by potentially tetradentate mixed iminophosphorane ligands were shown to catalyze the transfer hydrogenation reactions of acetophenone in isopropanol at reflux.[53] More recently, a $Fe^{II}$-H complex supported by an amido-iminophosphorane was used as a precatalyst for the hydrodefluorination of aromatics in presence of silanes.[46]

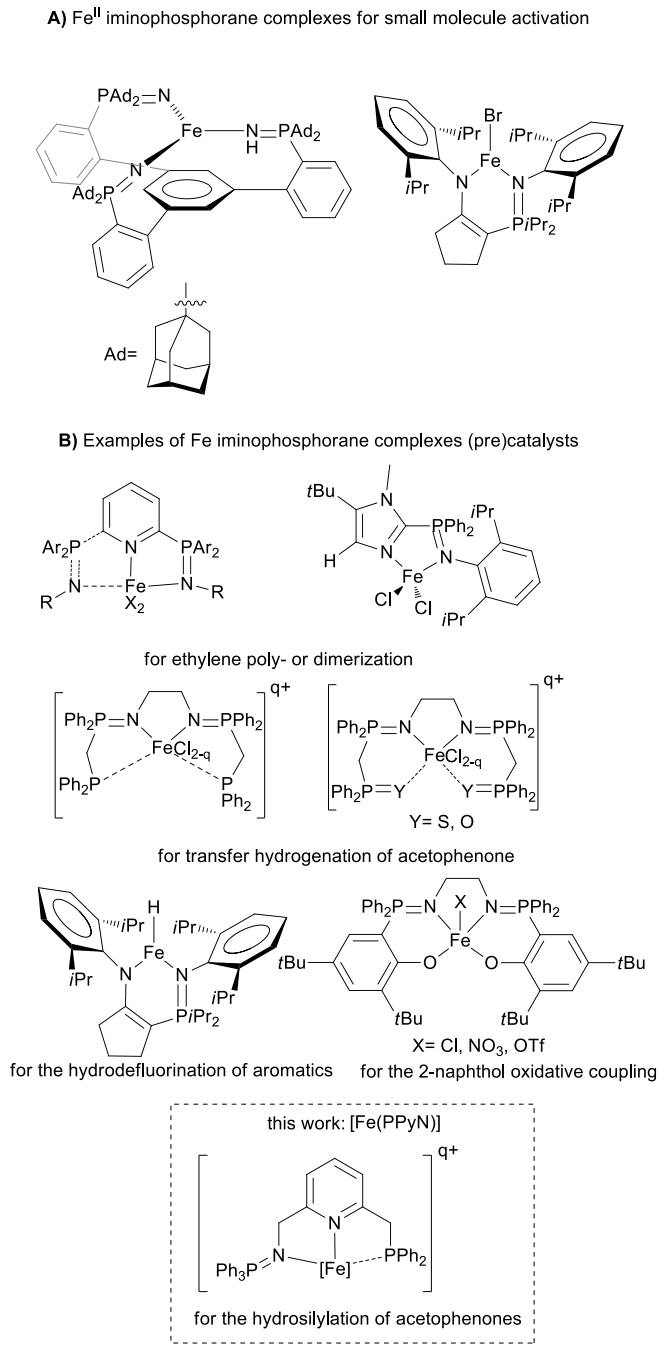


Figure 3: Fe iminophosphorane complexes used for stoichiometric and catalytic reactions

Finally, phosphasalen iron(III) complexes were shown to realize the catalytic oxidative coupling of 2-naphtol.[54] Among these limited examples only one associates the iminophosphorane with soft phosphine donors. We previously synthesized a tridentate (P,N,N) ligand (hereafter labelled PPyNP) combining an iminophosphorane and a phosphine arranged around a lutidine core and studied its coordination to noble metals (Pd and Ru).[55, 56] We were curious to investigate its coordination to $Fe^{II}$ and report here the synthesis of neutral and cationic iron complexes supported by this PPyNP ligand, studies of their deprotonation and the introduction of strong field isocyanide ligands, as well as the room temperature catalytic hydrosilylation of acetophenones using a catalyst generated *in situ* from cationic $Fe^{II}$ complexes and $KHBEt_3$.

## Results and discussion

The previously described PPyNP ligand[55] was synthesized as its LiCl adduct and coordinated in THF to $FeCl_2$ (Scheme 1). After stirring overnight at room temperature, the reaction mixture deposited a yellow precipitate. This was collected and washed with THF to provide $[Fe(PPyNP)Cl_2]$ (**1**) in 62% yield. The complex is paramagnetic and therefore exhibits no detectable $^{31}P\{^1H\}$ NMR signal. Its $^1H$ NMR spectrum shows broad signals that are both highly shielded and deshielded (at 230, 60, and -62 ppm see Figure S1). The magnetic moment of **1** in solution using the Evans methodology[57] was found to be 4.8 $\mu_B$, which indicates a high-spin $Fe^{II}$ complex (S= 2).

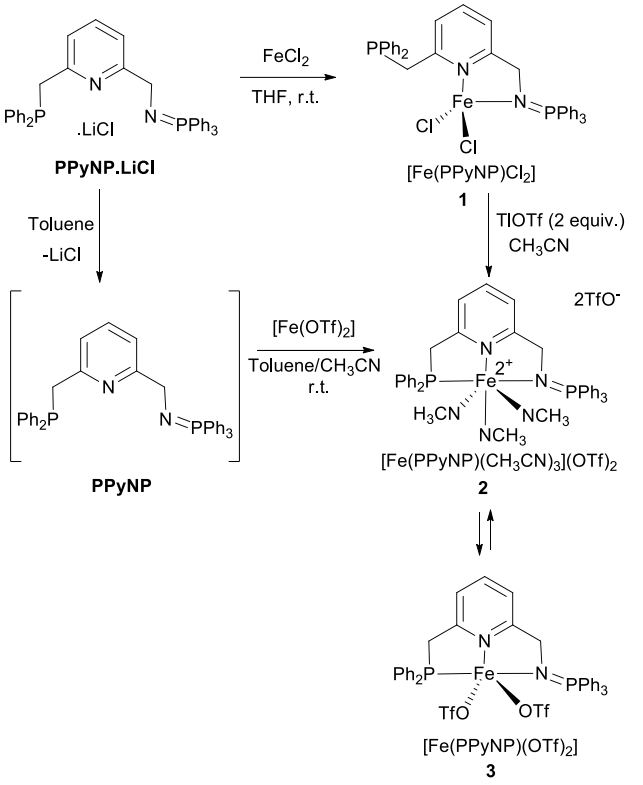


Scheme 1: Synthesis of $Fe^{II}$ complexes supported by the PPyNP ligand

The structure of **1** was elucidated by X-ray diffraction (Figure 4). The iron center presents a distorted tetrahedral geometry ($\tau_4$ = 0.85),[58] where only the 2 nitrogen atoms of the ligand are coordinated. The formation of the 5-membered metallacycle accounts for the deformation which is reflected in the acute N2-Fe-N1 angle (80.66°). The P=N bond length measured at 1.607 Å is elongated compared to free iminophosphoranes as generally observed upon metal coordination.‡ The phosphine group is clearly oriented away from the metal. The observed structural parameters support the anticipated preference of the

"hard" $Fe^{II}$ of the iminophosphorane ligand over the "softer" phosphine.[59]

Figure 4: X-ray structure of $[Fe(PPyNP)Cl_2]$ (**1**) (with thermal ellipsoids drawn at the 50% probability level). The H atoms and one THF molecule are omitted for

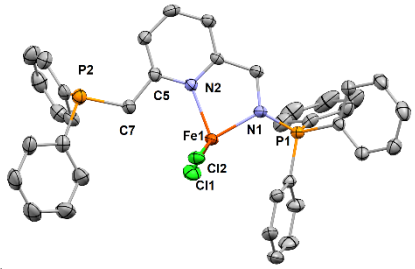


clarity. Selected bond lengths [A] and angles [°]: Fe1-N1 = 2.041(3); Fe1-N2 = 2.101(3); Fe1-Cl1: 2.3155(12); Fe1-P2 = 2.510(2); P1–N1 = 1.607(3); P2–C7 = 1.837(4); C7-C5 = 1.504(5); N2–Fe1–P2 = 77.6(1); N1-Fe1-N2 = 80.58(11); N1-Fe1-Cl1 = 114.11(9); N1-Fe1-Cl2 = 118.90(9); Cl1-Fe1-Cl2= 120.10(4).

Reasoning that a pincer coordination mode should be favored in cationic complexes, chlorides were abstracted from **1** (Scheme 1, right). This reaction was carried out with thallium triflate, which has been previously employed in Milstein's group with iron PNN complexes[60] Upon addition of 2 equivalents of Tl(OTf) to an acetonitrile solution of **1**, the solution rapidly turned purple and a white precipitate of TlCl formed. The precipitate was filtrated off, and the solvent was evaporated to leave a pale solid. Analysis of the product by NMR spectroscopy gave little information; the absence of $^{31}P$ NMR signal pointed to the formation of paramagnetic compounds while the $^{1}H$ NMR spectrum (Figure S2) suggested the presence of a mixture, because we observed broad highly shielded or deshielded resonances (at -6.4, 12.0, 15.3, 40.1, and 53.5 ppm) together with some sharply-defined signals. The former were assumed to correspond to a paramagnetic compound and the latter to a diamagnetic one.

Consistently, under differing crystallization conditions, we were able to identify two different complexes $[Fe(PPyNP)(CH_3CN)_3](OTf)_2$ (**2**) and $[Fe(PPyNP)(OTf)_2]$ (**3**) by X-ray crystallography depending on the crystallization conditions. Upon slow evaporation of a benzene solution, small single crystals were formed. Their analysis by X-ray diffraction gave a low-quality structure that was sufficient to establish the formation of $[Fe(PPyNP)(OTf)_2]$ (**3**) where both triflates are bound to the metal. A higher quality structure of the same complex could be obtained following an alternative route (vide infra). On the other hand, crystals obtained by diffusion of diethyl ether into an acetonitrile solution of the residue led to the structure shown in Figure 5. In this structure the iron adopts a distorted octahedral geometry, where the PPyNP ligand occupies three meridional sites and the acetonitrile molecules take up the three remaining ones. The bond between Fe-N1 bond length of 2.060(14) Å is comparable to its homologue in **1** while the Fe-$N_{pyr}$ bond is slightly shorter (1.972(4) Å). The Fe-P distance of 2.2338(15) Å in **2** lies in the lower range of values reported in the CCDC for phosphine conlongertaining $[Fe(CH_3CN)_3]$ complexes. Compared to the same references, the Fe-$NCCH_3$ bonds (1.92-1.93 Å) also are in the lower range of those already described.

To further investigate these triflate complexes we employed a different synthetic protocol that involved the direct coordination of $[Fe(OTf)_2]$ to a PPyNP ligand that had been freed from associated lithium chloride by extraction into toluene. The solution rapidly turned green and then purple after stirring 1 day at room temperature. The $^{1}H$ NMR spectrum resembled that obtained after chloride abstraction from **1** and pointed towards the presence of two complexes presumably those identified previously by X-ray diffraction analysis. We did not manage to determine their ratio by $^{1}H$ NMR spectroscopy. Nevertheless, we observed that the ratio between peaks varies as a function of the time that the mixture was left under vacuum, which suggests that these complexes are in equilibrium. The color of the product mixture changed accordingly, with longer drying giving a paler product. Unfortunately, we always isolated a mixture of both compounds that were formed in a minimal yield of 65%.

Figure 5: X-ray structure of $[Fe(PPyNP)(CH_3CN)_3](OTf)_2$ (**2**) with thermal ellipsoids

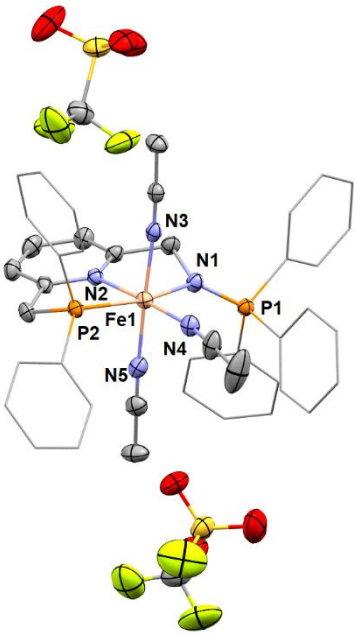


(drawn at the 50% probability level). The H atoms are omitted and the phenyl rings are represented in the wireframe mode for clarity. Selected bond lengths [Å] and angles [°]: [LFe(CH3CN)3](OTf)2 Fe1-N1 = 2.060(4); Fe1-N2 = 1.972(4); Fe1-P2 = 2.2338(15); Fe1-N3: 1.932(5); Fe1-N4 = 1.933(5); Fe-N5 = 1.925(5); P1–N1 = 1.589(4); N2–Fe1–P2 = 83.32(12); N2-Fe1-N1 = 81.77(17); N4-Fe1-P2 = 94.14(13); N4-Fe1- N1= 100.85(17); N4-Fe1- N1; N5-Fe1-N3: 177.0(2)

A higher quality X-ray structure of **3** could be obtained from crystals grown by the diffusion of pentane vapour into a benzene solution of the complexes. It is presented in Figure 6. The iron is coordinated by the PPyNP ligand in a tridentate fashion and the triflates complete the coordination sphere. To assign the geometry of the iron in this complex we rely on the $\tau_5$ index[61] ($\tau_5$= 1 for an ideal trigonal bipyramid, 0 for an ideal square based pyramid) whose calculated value of 0.61 implies that the geometry, even if highly distorted, is closer to a trigonal bipyramid. The apical positions of the trigonal bipyramid are occupied by the N atom of the pyridine ring and an O from a triflate (O1-Fe1-N2 172.49(6)). The basal plane consists of the phosphorus P2, the iminophosphorane N1, and O4 from the second triflate, but these atoms are not coplanar with the metal, the P2 atom lying (0.971 Å) above the mean plane defined by Fe1, O4, and N1. The angles between these atoms are also far from the ideal 120° value; the N1-Fe1-P2 angle is wider (135.87(4) °) while the O4-Fe1-N1 and O4-Fe1-P2 are

more acute (113.88(6) and 103.61(5) ° respectively). The Fe-N2 and Fe-P2 bonds are shorter in **2** compared to **3** while the Fe1-N1 ones are comparable (Table S3). This is consistent with a stronger coordination of the PPyNP ligand in the dicationic octahedral complex.

Figure 6: X-ray structure of $[Fe(PPyNP)(OTf)_2]$ (**3**) Fe1-N1 = 2.0499(15); Fe1-N2 = 2.1972(14); Fe1-O1 = 2.0690(13); Fe1-O2: 2.0439(14); Fe1-P2 = 2.4733(5); P1–N1

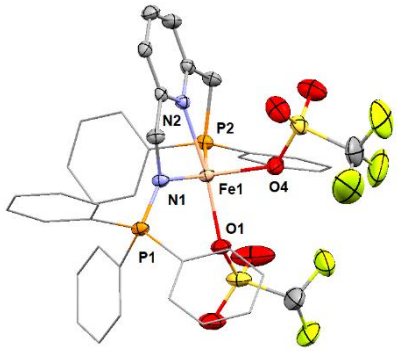


= 1.6097(15); N2–Fe1–P2 = 75.90(4); N2-Fe1-N1 = 76.63(5); O1-Fe1-P2 = 106.82(4); N1-Fe1-O1= 97.04(6) O1-Fe1-N2: 172.49(6).

We then investigated the introduction of strong field ligands and focused on isocyanide[62, 63] because, unlike CO, it cannot enter deleterious aza-Wittig reactions with the iminophosphorane moiety and it can also be conveniently introduced with well- controlled stoichiometry. The addition of tertbutylisocyanide to **1** was followed by NMR monitoring. It showed that the same diamagnetic compound formed irrespective of the number of equivalents used (1, 2, or 3).

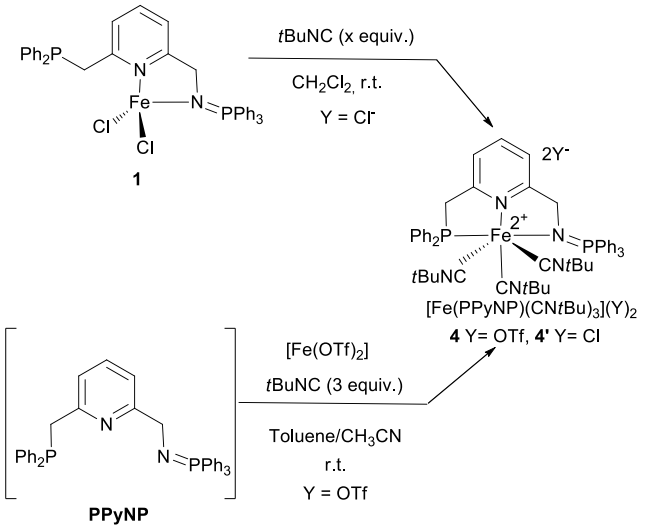


Scheme 2: Access to **$[Fe(PPyNP)(CNtBu)_3]^{2+}$** complexes

This diamagnetic complex exhibited two phosphorus doublet resonances around 74 and 46 ppm and these are assigned to the $P^{III}$ and $P^{V}$ nuclei respectively ($J_{P,P}$ = 5.5 Hz). The coordination of three isocyanide ligands was confirmed by $^1H$ NMR spectroscopy as well as X-ray diffraction analysis (vide infra). The addition of *t*BuNC to a mixture of PPyNP and $Fe(OTf)_2$ also led to the coordination of three isocyanide whatever the quantity of reagent introduced allowing to isolate $[Fe(PPyNP)(CNtBu)_3](OTf)_2$ (**4**) in 85% yield. In this complex the isocyanide groups are characterized by two singlets $^1H$ resonances at 1.21 and 1.00 ppm in $CD_2Cl_2$ that integrate respectively for 18 and 9 H. Similarly, the quaternary isocyanide carbons give rise to two $^{13}C$ resonances at 164.1 and 159.8 ppm. The crystal structure of **4'** is shown in Figure 7. The iron exhibits an octahedral geometry with the meridional coordination of the pincer PPyNP ligand and also that of the three isocyanides, one of which is in the meridional plane. N2, P2, N1, C8, and Fe1 are almost coplanar (distance Fe1-median plane 0.038 Å), while the two apical isocyanides are orthogonal to the P2-N2-N1-C8 plane. On the contrary the pyridine is slightly tilted away from this plane (deviation angle 19.34°). In terms of bond lengths, a comparison between the tris(isocyanide) (**4'**) and tris(acetonitrile) complex (**2**) (Table S3) shows that the P-N, N1-Fe, and Fe-Npyr bonds are similar while the Fe-P2 is shorter in the isocyanide complex (2.2035(8) vs 2.2338(15) Å).

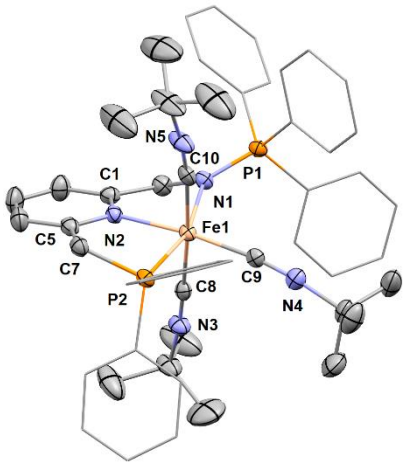


Figure 7. X-ray structure of $[Fe(NPyNP)(CNtBu)_3]Cl_2$ (**4'**) with thermal ellipsoids (drawn at the 50% probability level). The H atoms and the Cl- anions are omitted and the phenyl rings represented in the wireframe mode for clarity. Selected bond lengths [Å] and angles [°]: Fe1-N1 = 2.055(2); Fe1-N2 = 1.992(2); Fe1-P2 = 2.2035(8)); Fe1-C8: 1.854(3); Fe1-C9 = 1.889(3); Fe1-C10 = 1.899(3);P1–N1 = 1.604(2); N2–Fe1–P2 = 83.60(7); N2-Fe1-N1 = 79.27(10); C8-Fe1-P2 = 95.92(9); C8-Fe1-N2= 101.65(11); C9-Fe1-C10= 175.89(12).

The metal-ligand cooperation upon deprotonation of the phosphinomethyl group and the subsequent dearomatization of the pyridine, has been investigated within iron complexes supported by bis(phosphinomethyl)-pyridine (PNP)[64] and -phenantroline (PNNP) ligand.[65] To the best of our knowledge, studies with PNN ligands are restricted, to bipyridine based ligand[66] and phosphine α-iminopyridine ones.[67] In particular, the deprotonation of phosphino-lutidine-amine (PNN) Fe complexes has not been reported yet. Given that we have already investigated the deprotonation α to the pyridine in the PPyNP supported Ru complexes, we investigated the deprotonation of the $Fe^{II}$ complexes we prepared (Scheme 3).

As we had previously observed with Ru complexes, the addition of one equivalent of potassium hexamethyldisilazane (KHMDS) to a THF or toluene solution of **1**, caused the reaction to darken. The product could not be isolated and decomposed upon removal of the solvent, whilst its paramagnetism precluded an investigation by NMR spectroscopy. Nevertheless, when the deprotonation was carried out in toluene in presence of pyridine, single crystals could be obtained by diffusion of petroleum ether into the reaction mixture.

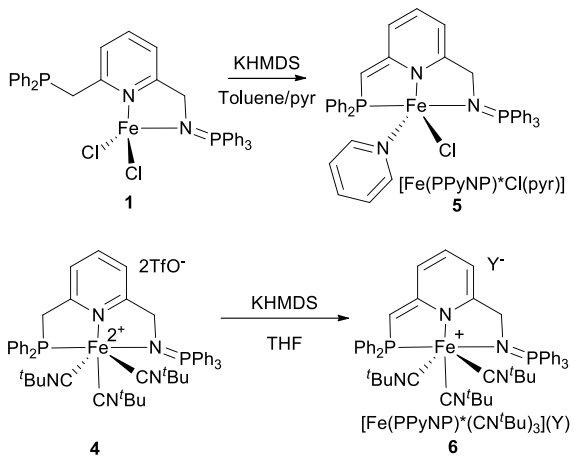


Scheme 3: Deprotonation of **PPyPN** supported Fe$^{II}$ complexes

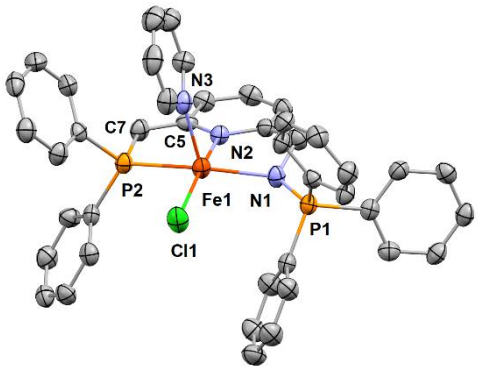


Figure 8. X-ray structure of [Fe(PPyNP)*Cl(pyr)] (**5**) (with thermal ellipsoids drawn at the 50% probability level). The H atoms are omitted for clarity. Selected bond lengths [Å] and angles [°]:Fe1-N1 = 2.153(3); Fe1-N2 = 2.137(3); Fe1-N3 = 2.176(3); Fe1-Cl1: 2.3155(12); Fe1-P2 = 2.5098(12); P1–N1 = 1.590(3); P2–C7 = 1.750(4); C7-C5 = 1.389(6); N2–Fe1–P2 = 77.57(9); N2-Fe1-N1 = 77.76(12); N1-Fe1-Cl1 = 103.45(9); Cl1-Fe1- P2= 96.48(4).

Their X-ray diffraction analysis revealed the formation of [Fe(PPyNP)*Cl(pyr)] (**5**) (Figure 8). The geometry of the Fe is square pyramidal ($\tau_5$= 0.25) with the PPyNP ligand present as a pincer, alongside a pyridine, and a chloride. The coordination of the phosphine is probably triggered by the loss of a chloride ligand that accompanies the dearomatization of the pyridine. The iron center lies out of the P2N2N1 plane by 0.410 Å and is located in the hemisphere containing the pyridine ligand, which is not orthogonal to this meridional plane (angle 75.43 °). The deprotonation at the phosphinomethyl position is shown by a shortening of the C7-C5 bond to 1.389(6) Å in **5** *vs* 1.505 Å in **1** and a gain in planarity of the molecule. As a result, C5, C7, and P2 are almost coplanar with the aromatic ring (deviation 1.33 °). The alternation of short and long bonds in the pyridine ring reflects its dearomatization following the deprotonation as previously observed.[66, 68, 69] The coordination of the phosphine arm induces an elongation of both Fe-N2 and Fe-N1 bond lengths when compared to **1**. They measure respectively 2.101(3) and 2.043(3) Å in the dichloride complex **1** *vs* 2.137(3) and 2.153(3) Å in the monochloride complex **5**. The addition of KHMDS to a solution containing a mixture of complexes **2** and **3** complexes also led a color change. Nevertheless, we could not investigate further this reaction; NMR spectroscopy was inconclusive and we were unable to grow crystals. Monitoring of the deprotonation reaction was easier when starting from **4** (Scheme 3). The addition of KHMDS induced a color change from brown to red and the $^{31}P\{^1H\}$ NMR spectrum of the reaction mixture showed the formation of a new complex characterized by two doublets at 59.6 and 40.4 ppm ($J_{P,P}$ = 6.0 Hz). Attempts to isolate this complex failed, with the evaporation of the volatiles leading repeatedly to a partial reprotonation (Figure S9). However, the formed complex was characterized by *in situ* NMR spectroscopy. The $^1H$ NMR spectrum showed 3 signals integrating for 1 H at 6.73, 6.39, 5.57 ppm that are consistent with resonances of the dearomatized pyridine protons. Two other signals integrating respectively for 2 and 1 protons that were observed at 3.89 and 3.81 ppm may be assigned to the unchanged and deprotonated benzylic position respectively.

We were then interested in forming Fe-H complexes by incorporating hydrides into the different iron complexes prepared i.e. **1**, **2/3,** and **4**. We used various hydride donors: $NaBH_4$, $LiAlH_4$, or $KHBEt_3$, in MeOH for the first one and THF for the others. Starting from cationic triflate complexes (**2** and **3**), we also performed the addition of the hydride donor after overnight drying in vacuo in order to eliminate the acetonitrile. $NaBH_4$ was not reactive enough to induce a reaction but in all other cases the addition of the hydride source induces a strong color change. However, no complexes could be isolated or identified by X-ray crystallography, while their paramagnetic NMR spectra did not allow to get any indication regarding their structure. Reasoning that those two classes of complexes (i.e. PPyNP supported Fe-H and (PPyNP)* supported Fe ones) may be too sensitive to be isolated but may be competent as *in situ* generated catalysts we tested two catalytic reactions.

The first, the deshydrogenative coupling of hexan-1-ol was attempted with a catalytic amount of complexes **1**, **2/3**, or **4** but no conversion was observed (Scheme S1). It was suspected that the lack of reactivity might reflect a lower Lewis acidity of the iron center in these complexes when compared with literature iron catalysts that are competent for similar reactions. Such complexes do not feature electron rich iminophosphorane ligand and generally incorporate at least one π accepting CO.[70] The Lewis acidity of the metal center is important during the first steps of the catalysis, where increased Lewis acidity can be expected to favor coordination of the alcohol and hydride transfer to the metal. However, electron rich metal centers are generally an asset when tackling reduction processes. We therefore investigated whether an *in situ* generated PPyNP supported iron hydride would be able to catalyze the hydrosilylation of acetophenones. We chose to avoid strong coordinating solvents and ions that may complicate the addition and therefore prepared the *in situ* catalyst ($[Fe]_{cat.}$) from PPyNP iron triflate complexes (**2**/**3**) that had been dried overnight in vacuo (Scheme 4). The obtained off-white solid was dissolved in THF leading to a green solution, the change of color being tentatively attributed to the formation of $[Fe(PPyNP)(THF)_3](OTf)_2$, which could not be characterized. Addition of two equivalents of $KHBEt_3$ was made in an attempt to demonstrate the presence of hydride complexes indirectly, through their reactivity. We first reacted this *in situ* generated iron complex with an equimolar quantity of acetophenone and

silane (either $Et_3SiH$, $Ph_2SiH$, or $PhSiH_3$) (Scheme 4). Phenylsilane was the most effective, and allowed a total conversion of the ketone into its silylether upon overnight stirring at room temperature. The reaction was monitored by $^1H$ NMR spectroscopy, by following the disappearance of the singlet corresponding to the $CH_3$ of the acetophenone ($\delta_H$(THF-$d_8$)= 2.5 ppm) and the appearance of a doublet corresponding to the same group in the silylether ($\delta_H$(THF-$d_8$)= 1.38 ppm). No corresponding change was observed when the same transformation was attempted without the iron complex.

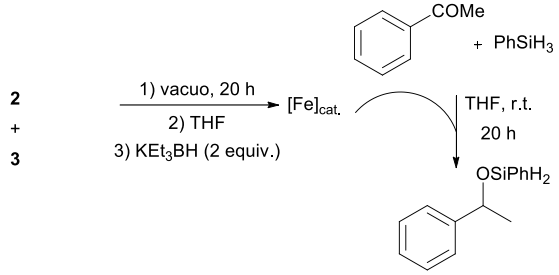


Scheme 4: *In situ* generation of the active Fe complex enabling stoichiometric hydrosilylation of acetophenone

After this encouraging observation, we explored different catalytic conditions. In each case, the O-Si bond in the product was cleaved quantitively in basic methanol, and the catalytic conversion was determined by $^1H$ NMR spectroscopy through integrating the product alcohol against trimethoxybenzene internal standard (Table 1). Conducting the reaction with 5 mol % catalyst at room temperature gave a quantitative formation of alcohol after both 24 or 2 h (Table 1, entries 1-2). Decreasing the catalyst amount to 1 mol % required longer reaction times, with 81% formation of alcohol after a day. (Table 1, entries 2-3). Raising the temperature from 20° to 40°C, increased the NMR yield from 12 to 88% after 2 h but only 23% completion was observed at 40°C after 1 h. Heating allowed to decrease the reaction time without significantly affecting the yield, therefore we evaluated other acetophenones at room temperature. Surprisingly, acetophenones with an electron donor group led to a quantitative conversion, while the presence of an electron poor substituent led to slightly lower yields. Generally, the reaction is more efficient with electron poor ketones which is rationalized in terms of an easier insertion of the C=O into the M-H bond. Here the coordination of the ketone or the regeneration of the active catalyst via the formation of the O-Si, may be the more difficult steps.[71] We could not investigate this point further because we could not determine the nature of the precatalyst. The reaction worked well with the substituted p- and m-acetophenones but the lack of any reaction with o-Me derivative implies that the catalyst is highly sensitive to steric hindrance. Note that the alcohol derived from 3-pyridinecarboxaldehyde formed in 57%.

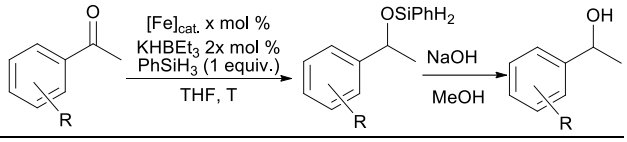


| Entry | R | Time (h) | mol % Catalyst | T (°C) | NMR Yield (%)[a] |
|---|---|---|---|---|---|
| 1 | H | 24 | 5 | r.t. | 100 |
| 2 | H | 2 | 5 | r.t. | 100 |
| 3 | H | 2 | 1 | r.t. | 12 |
| **4** | **H** | **24** | **1** | **r.t.** | **81** |
| 5 | H | 2 | 1 | 40 | 88 |
| 6 | H | 1 | 1 | 40 | 23 |
| 7 | H | 2 | 1 | r.t. | 88 |
| 8 | 4-OMe | 24 | 1 | r.t. | 100 |
| 9 | 4-$NMe_2$ | 24 | 1 | r.t. | 100 |
| 10 | 3-Me | 24 | 1 | r.t. | 100 |
| 11 | 4-CN | 24 | 1 | r.t. | 88 |
| 12 | 4-F | 24 | 1 | r.t. | 82 |
| 13 | 4-$CF_3$ | 24 | 1 | r.t. | 74 |
| 14 | 2-Me | 24 | 1 | r.t. | 0 |

[a] using $(OMe)_3$-$C_6H_4$ as internal reference

Table 1: Catalytic Hydrosilylation of acteophenones

No conversion was observed for methylbenzoate, benzamide nor N,N dimethylbenzamide. Taken together the performances of this *in situ* generated catalyst is competitive with other pincer ligand based iron hydrosilylation catalysts.[72, 73] Better performances have also been reported,[74, 75] but in these cases the iron has either a lower oxidation state or does not exhibit an octahedral geometry. Nevertheless, this is the first example of an iron complex supported by an iminophosphorane ligand active for the hydrosilylation of acetophenones and the conversions observed are comparable to those described for the hydrogenation of acetophenones with bisphosphinomethylpyridine (PNP) iron complexes.[64]

## Conclusions

We have described the synthesis of iron(II) complexes supported by a phosphine-lutidine-iminophosphorane ligand (PPyNP). We isolated the neutral tetrahedral [Fe(PPyNP)$Cl_2$] (**1**) complex exhibiting a $\kappa^2$-N,N coordination mode as well as the cationic octahedral [Fe(NPyNP)$(CNtBu)_3]X_2$ (X = OTf (**4**), Cl (**4'**)) where the PPyNP ligand coordinates as a pincer. When using less coordinating triflate anion a mixture of solvated (**2**) and unsolvated (**3**) complexes formed which could not be thoroughly characterized. We investigated the fate of PPyNP supported $Fe^{II}$ complexes upon deprotonation and showed that both **1** and **4** underwent deprotonation at the phosphinomethyl position. We also attempted the synthesis of M-H complexes, which proved elusive. While these complexes are not precatalyst for the dehydrogenative coupling of hexan-1-ol, an iron complex generated *in situ* from the triflate complexes (**2** and **3**) catalyzed the hydrosilylation of acetophenones at room temperature within 1 day at 1 mol % loading. This strengthens the idea that iminophosphoranes may be good candidates for developing iron-based reduction catalysts but further ligand

design is necessary to improve the reactivity of the complexes. Work in that direction will be pursued in our laboratory.

## Experimental part

**Synthesis**

All reactions were conducted under an atmosphere of dry nitrogen, or argon, using standard Schlenk and glovebox techniques. Solvents were dried with a M-Braun MB-SPS 800 solvent purification system and THF was distilled over Na and benzophenone. The deuterated solvents were stored over activated molecular sieves. All other reagents and chemicals were obtained commercially and used without further purification. Nuclear Magnetic Resonance (NMR) spectra were recorded on a Bruker Avance 300 spectrometer operating at 300 MHz for $^{1}$H, 75.5 MHz for $^{13}$C and 121.5 MHz for $^{31}$P. Solvent peaks were used as internal references for $^{1}$H and $^{13}$C{$^{1}$H} chemical shifts (ppm). $^{31}$P{$^{1}$H} NMR spectra are relative to an 85% $H_3PO_4$ external reference. Unless otherwise mentioned, NMR spectra were recorded at 300 K. Additional information were obtained from COSY, HSQC, and HMBC experiments. Coupling constant are expressed in hertz. The following abbreviations are used: br, broad; s, singlet; d, doublet; q: quadruplet; t, triplet; m, multiplet; v, virtual. The spectra were analyzed with MestReNova software. IR spectra were recorded on an IR-TF Thermo Scientific Nicolet iS5 spectrometer. Mass spectrometry experiments were recorded on tims-TOF mass spectrometer (Bruker, France). The PPyNP ligand was synthesized according to the previously published procedure.[55]

*Synthesis of dichloro(6-[(diphenylphosphino)methyl]-N-(triphenylphosphoranylidene)-2-pyridinemethanamine-κP,N$^2$-)iron(II) [Fe(PPyNP)Cl$_2$] **1***: PPyNP.LiCl (365.4 mg, 0.6 mmol) and $FeCl_2$ (126.8 mg, 0,6 mmol) were mixed in THF (8 mL) and stirred 16 h at room temperature. The slightly colored precipitate is filtered and washed with THF (3 x 8 mL) and pentane (5 mL). Volatiles were then removed in vacuo to yield **1** as a pale greenish powder (254 mg, 0.37 mmol, 62 %). Single crystals were grown by diffusion of pentane into a dichloromethane solution of the complex. $\mu_{eff}$ = 4.8 μB (by the Evans' method in $CD_2Cl_2$). HRMS (ESI$^+$): m/z: [**1**-Cl]$^+$ calcd 657.1074 for $C_{37}H_{32}ClFeN_2P_2^+$; Found 657.1063.

*Preparation of tris(acetonitrile)(6-[(diphenylphosphino)methyl]-N-(Triphenylphosphoranylidene)-2-pyridinemethanamine-κP,N,N$^3$)iron(II) ditriflate [LFe(CH$_3$CN)$_3$](OTf)$_2$ (**2**) and (6-[(Diphenylphosphino)methyl]-N-(Triphenylphosphoranylidene)-2-pyridinemethanamine-κP,N,N$^3$)ditriflateiron(II) [Fe(NPyNP)(OTf)$_2$] (**3**)*: PPyNP.LiCl (0.243 g, 0.428 mmol) was placed in toluene (2 x 2 mL) to remove the LiCl salt by filtration. A solution of $Fe(OTf)_2$ (0.151 g, 0.428 mmol) in acetonitrile (2 mL) was then added dropwise to the NPPyNP toluene solution. The mixture took a red color evolving to an orange color after 24 hours stirring. The volatiles were evaporated to yield an orange solid (0.283 g, 0.28 mmol (pure **2**)-0.31 mmol (pure **3**) 65-72%). Single crystals of **2** were grown at room temperature by diffusion of vapours of pentane into a concentrated acetonitrile solution of the complexes (c~10 mg/mL). Single crystals of **3** were grown at room temperature by diffusion of pentane vapours into a concentrated benzene solution of the complexes in the glovebox (c~10 mg/mL).

*Synthesis of (6-[(diphenylphosphino)methyl]-N-(triphenylphosphoranylidene)-2-pyridinemethanamine-κP,N,N$^3$)tris(tertbutylisocyanide)iron(II) ditriflate [Fe(PPyNP)(CNtBu)$_3$](OTf)$_2$ (**4**)*: PPyNP.LiCl (0.03 g, 0.05 mmol) was placed in toluene (3 x 1 mL) to remove the LiCl salt by filtration. The yellow filtrate was used directly for the next step. A solution of $Fe(OTf)_2$ (0.017 g, 0.05 mmol) in acetonitrile (3 mL) was added to the toluene filtrate and then CN$^t$Bu (0.15 mmol, 3 equiv., 17 μL). The reaction was stirred for 24 h at room temperature, the volatiles were removed and the residue was washed with diethyl ether (2 mL) leading to **4** as an orange solid (52 mg, 0.043 mmol, 85%). $^{31}$P{$^{1}$H} NMR ($CD_2Cl_2$): δ 73.8 ppm (d, $J_{P,P}$ = 5.5 Hz, P$^{III}$), 46.2 ppm (d, $J_{P,P}$ = 5.5 Hz, P$^{V}$). $^{1}$H-NMR ($CD_2Cl_2$) : δ 8.05 (m, 2 H, $CH_{Ar}$), 7.83-7.78 (m, 4 H, $CH_{Ar}$), 7.69-7.64 (m, 6 H, $CH_{Ar}$), 7.57-7.60 (m, 6 H, $CH_{Ar}$), 7.54-7.48 (m, 4 H, $CH_{Ar}$), 7.41-7.38 (m, 3 H, $CH_{Ar}$), 7.24 (dd, $J_{H,H}$= 7.5 and 6.5 Hz, 2H), 7.16 (m, 2 H, $CH_{Ar}$), 4.47 (d, $J_{P,H}$ = 11.0 Hz, 2 H, $CH_2$), 4.36 (d, $J_{P,H}$ = 10.5 Hz, 2 H $CH_2$), 1.21 (s, $CH_3$, 9 H), 1.00 (s, $CH_3$, 18 H). $^{13}$C{$^{1}$H} NMR (75.5 MHz, $CD_2Cl_2$): 164.9 (J not observed, C$^{IV}$), 160.5 (J not observed, C$^{IV}$), 140.4 (s, $CH_{Ar}$), 138,6 (s, C$^{IV}$), 134.6 (d, $J_{P,C}$ = 3.0 Hz $CH_{Ar}$), 134.1 (d, $J_{P,C}$ = 10.0 Hz, $CH_{Ar}$), 133.3 (d, $J_{P,C}$ = 46.0 Hz, C$^{IV}$), 132.8 (d, $J_{P,C}$ = 2.5 Hz, $CH_{Ar}$), 132.3 (d, $J_{P,C}$ = 10.0 Hz, $CH_{Ar}$), 130.4 (d, $J_{P,C}$ = 12.0 Hz, $CH_{Ar}$), 130.2 (d, $J_{P,C}$ = 10.5 Hz, $CH_{Ar}$), 129.6 (s, $CH_{Ar}$), 128.8 (s, $CH_{Ar}$), 127.0 (d, $J_{P,C}$ = 100.0 Hz, C$^{IV}$), 125.9 (s, $CH_{Ar}$), 123.9 (d, $J_{P,C}$ = 10.0 Hz, $CH_{Ar}$), 120.0 (s, $CH_{Ar}$), 61.1 (s, $CH_2$), 60.4 (d, $J_{P,C}$ = 5.5 Hz Hz, C$^{IV}$), 44.5 (d, $J_{P,C}$ = 31.0 Hz, $CH_2$), 30.9(s, $CH_3$), 30.2 (s, $CH_3$). HRMS (ESI$^+$): m/z: [Fe(NPyNP)(CN*t*Bu)$_3$(OTf)]$^+$ calcd 1020.3115 for $C_{53}H_{59}F_3FeN_5O_3P_2S^+$; Found 1020.3110, [Fe(NPyNP) (CN*t*Bu)$_3$]$^+$ calcd 871.3595 for $C_{52}H_{59}FeN_5P_2^+$;Found 871.3544; [LFe(NPyPN)(CN*t*Bu)$_3$]$^{2+}$ calcd 435.6798 for $C_{52}H_{59}FeN_5P_2^{2+}$; Found 435.6796; [Fe(NPyNP)]$^{2+}$ calcd 311.0695 for $C_{37}H_{32}FeN_2P_2^{2+}$; Found 311.0694, : [Fe(NPyNP)(CN*t*Bu)]$^{2+}$ calcd 352.6063 for $C_{42}H_{41}FeN_3P_2^{2+}$; Found 352.6053. IR ($CH_3CN$, cm$^{-1}$): 2986,2940, 2153, 2145, 1437, 1373, 1266, 1224.

*Preparation of chloro(6-[(diphenylphosphino)methylene]-N-(triphenylphosphoranylidene)-2-1,2-dihydropyridinatomethanamine-κP,N,N$^3$)pyridineiron(II) [Fe(NPyNP)*Cl(pyr)] (**5**):* KHMDS (14.3 mg, 0.07 mmol) was added to a solution of **1** (49.6 mg, 0.07 mmol) in a toluene (1.5 mL) containing pyridine (3 drops). Crystals were obtained by diffusion of petroleum ether into the crude mixture.

*Preparation of (6-[(diphenylphosphino)methylene]-N-(triphenylphosphoranylidene)-2-1,2-dihydropyridinatomethanamine-κP,N,N$^3$)tris(tertbutylisocyanide)iron(II) [Fe(NPyNP)*(CNtBu)$_3$](OTf) (**6**)*: KHMDS (6 mg, 0.03 mmol) was added to a solution of [Fe(NPyNP)(CNtBu)$_3$](OTf)$_2$ **4** (20 mg, 0.02 mmol) in THF-d$_8$, after stirring overnight at room temperature. The formation of [Fe(NPyNP)*(CNtBu)$_3$](OTf) (***6***): was ascertained by NMR spectroscopy. $^{31}$P{$^{1}$H} NMR (THF-d$_8$): δ 59.6 ppm (d, $J_{P,P}$ = 5.0 Hz, P$^{III}$), 40.4 ppm (d, $J_{P,P}$ = 5.0 Hz,P$^{V}$). $^{1}$H-NMR (THF-d$_8$) : δ 7.85 (m, 6 H, $CH_{Ar}$), 7.72 (m, 6 H, $CH_{Ar}$), 7.63 (m, 3 H, $CH_{Ar}$), 7.48 (m, 2 H, $CH_{Ar}$), 7.33 (m, 6 H, $CH_{Ar}$ ), 7.21 (d, $J_{H,H}$= 6.0 Hz, 1 H, $CH_{Ar}$), 7.16 (d, $J_{H,H}$= 8.0 Hz, 1 H, $CH_{Ar}$), 6.73 (m, 1 H, $CH_{pyr}$), 6.39 (d, $J_{H,H}$= 8.5 Hz, 1 H, $CH_{pyr}$), 5.57 (d, $J_{H,H}$= 8.5 Hz, 1 H,

$CH_{pyr}$) 3.88 (d, $J_{P,H}$= 10.0 Hz, 2 H, $CH_2$), 3.81 (s, 1 H, CH), 1.25 (s, $CH_3$, 9 H), 1.02 (s, $CH_3$, 18 H). $^{13}C\{^1H\}$ NMR (75.5 MHz, $CD_2Cl_2$): 169.9 (J not observed, $C^{IV}$), 158.7 (J not observed, $C^{IV}$), 140.4 (d, $J_{P,C}$= 48.0 Hz, $C^{IV}$), 136,7 (s, $C^{IV}$), 132.6 (d, $J_{P,C}$ = 9.5 Hz $CH_{Ar}$), 132.1 (d, $J_{P,C}$ = 2.5 Hz, $CH_{Ar}$), 131.6 (s, $CH_{Ar}$), 130.5 (d, $J_{P,C}$ = 9.0 Hz, $CH_{Ar}$), 128.3 (d, $J_{P,C}$ = 12.0 Hz, $CH_{Ar}$), 127.6 (d, $J_{P,C}$ = 4.0 Hz, $CH_{Ar}$), 127.3 (d, $J_{P,C}$ = 12.0 Hz, $CH_{Ar}$), 127.1 (s, $CH_{Ar}$), 127.0 (s, $CH_{Ar}$), 126.8 (d, $J_{P,C}$ = 9.5 Hz, $CH_{Ar}$), 124.2 (s, $C^{IV}$), 118.3 (J not observed, $C^{IV}$), 110.1 (d, J = 18.0 Hz, CH), 96.4 (s, CH), 57.8 (d, $J_{P,C}$ = 2.5 Hz Hz, CH), 57.2 (s, $C^{IV}$) 56.6 (s, $CH_2$), 29.0 (s, $CH_3$), 28.3 (s,$CH_3$).

**General protocol for the catalytic hydrosilylation of acetophenones**

A stock solution of the precatalyst was prepared from PPyNP.LiCl: PPyNP.LiCl (0.182 g, 0.322 mmol) was washed with toluene (2*2 mL) to remove the lithium salt. Dropwise addition of an acetonitrile solution of $Fe(OTf)_2$ (0.113 g, 0.322 mmol, 2 mL) to the toluene ligand solution led to a red colored solution turning orange after stirring 24 h at room temperature. The volatiles were evaporated and dried in vacuo under gentle heating (30-40°C) overnight to yield an off-white solid (**2/3**). The latter was dissolved in THF (4.25 mL) leading presumably to $[Fe(NPyNP)(THF)_3](OTf)_2$ to which 2 equivalents of $KHBEt_3$ were added to afford after 12 h stirring at room temperature a stock solution of the precatalyst with a concentration of 7.58 $10^{-2}$ $mol.L^{-1}$ assuming a total conversion.

Catalysis was performed by mixing solutions of $SiH_3Ph$ (98 μL of a 1.02 $mol.L^{-1}$ THF solution, 0.1 mmol, 1 equiv.) and acetophenone (54.6 μL of a 1.83 $mol.L^{-1}$ THF solution, 0.1 mmol, 1 equiv.), followed by the addition of a precatalyst solution (1 to 10 mol%, 0.01 to 0.001 mmol, i.e 132 or 13 μl of stock solution). The reaction mixture was stirred for the indicated reaction time at the given temperature. Then, the reaction was stopped by adding MeOH (1 mL) and an aqueous solution of NaOH (2M, 0.2 mL). Stirring was pursued for 1 h. The resulting mixture was then extracted with $Et_2O$ (3 x 2 mL) the organic phase was dried over $MgSO_4$ and filtered. The internal standard, trimethoxybenzene (16.1 mg, 0.1 mmol,1 equiv.) was added before removal of volatiles. Then resulting sample was dissolved in $CDCl_3$ and analyzed by $^1H$ NMR spectroscopy.

**X-ray crystallography**

Data were collected at 150 K on a Bruker Kappa APEX II diffractometer using a Mo-κ (λ = 0.71069Å) X-ray source and a graphite monochromator. The crystal structures were solved using Shelxt[76] or olex[77] and refined using Shelxl-97 or Shelxl-2014.[78] ORTEP drawings were made using ORTEP III[79] for Windows. Details of crystal data and structure refinements are summarized in Tables S1-2.

## Conflicts of interest

There are no conflicts to declare.

## Acknowledgements

The authors thank Ecole polytechnique and CNRS for financial support. They are grateful to Dr. Sophie Bourcier for mass spectrometry measurements, Marie Cordier for recording the X-ray structures of **2** and **4'**, and Dr. Duncan Carmichael for helping improve the text. GDR phosphore is also acknowledged for gathering the community of P-chemist in France.

## Notes and references

‡ The short P=N bond length in iminophosphorane is due to the stabilization of the electron density on the N atom by negative hyperconjugation i.e overlap between spx and σ*(P-C) orbitals. Upon coordination this phenomenon decreases leading to a lengthening of the PN bond and an elongation of the P-C ones. This can be observed with various examples; some examples can be found in those references.[80-92]

1. See references cited in this theme issue A. J. L. Pombeiro, *Dalton Trans.*, 2019, **48**, 13904-13906.
2. B. M. Atia, A. K. Sakr, M. A. Gado, H. S. El-Gendy, N. M. Abdelazeem, E. M. El-Sheikh, M. Y. Hanfi, M. I. Sayyed, J. S. Al-Otaibi and M. F. Cheira, *Polymers*, 2022, **14**, 1687.
3. J. Chakraborty, I. Nath and F. Verpoort, *Coord. Chem. Rev.*, 2016, **326**, 135-163.
4. G. Pratviel, *Coord. Chem. Rev.*, 2016, **308**, 460-477.
5. J. J. D. Sacramento and D. P. Goldberg, *Acc. Chem. Res.*, 2018, **51**, 2641-2652.
6. S. Mondal, P. K. Naik, J. K. Adha and S. Kar, *Coord. Chem. Rev.*, 2019, **400**, 213043.
7. M. Costas, M. P. Mehn, M. P. Jensen and L. Que, *Chem. Rev.*, 2004, **104**, 939-986.
8. S. M. Hoelzl, P. J. Altmann, J. W. Kueck and F. E. Kuehn, *Coord. Chem. Rev.*, 2017, **352**, 517-536.
9. O. Y. Lyakin, K. P. Bryliakov and E. P. Talsi, *Coord. Chem. Rev.*, 2019, **384**, 126-139.
10. Y. Lyu and P. Scrimin, *ACS Catal.*, 2021, **11**, 11501-11509.
11. J. García-Álvarez, S. E. García-Garrido and V. Cadierno, *J. Organomet. Chem.*, 2014, **751**, 792-808.
12. S. E. García-Garrido, A. Presa Soto and J. García-Álvarez, in *Advances in Organometallic Chemistry*, ed. P. J. Pérez, Academic Press, 2022, vol. 77, pp. 105-168.
13. T. Tannoux and A. Auffrant, *Coord. Chem. Rev.*, 2023, **474**, 214845.
14. N. Liu, D. D. Liu, B. Liu, H. Zhang and D. M. Cui, *Polym. Chem.*, 2021, **12**, 1518-1525.
15. Z. H. Mou, B. Liu, X. L. Liu, H. Y. Xie, W. F. Rong, L. Li, S. H. Li and D. M. Cui, *Macromolecules*, 2014, **47**, 2233-2241.
16. C. A. Wheaton and P. G. Hayes, *Catal. Sci. Technol.*, 2012, **2**, 125-138.
17. Z.-X. Wang and L. Wang, *Chem. Commun.*, 2007, 2423-2425.
18. L. Wang and Z.-X. Wang, *Org. Lett.*, 2007, **9**, 4335-4338.
19. A. Buchard, B. Komly, A. Auffrant, X. F. Le Goff and P. Le Floch, *Organometallics*, 2008, **27**, 4380-4385.
20. C. Zhang and Z. X. Wang, *Organometallics*, 2009, **28**, 6507-6514.
21. W. J. Guo and Z. X. Wang, *J. Org. Chem.*, 2013, **78**, 1054-1061.
22. Q. Zhang, X. Q. Zhang and Z. X. Wang, *Dalton Trans.*, 2012, **41**, 10453-10464.
23. D. J. Law and R. G. Cavell, *J. Mol. Catal.*, 1994, **91**, 175-186.
24. T. T. Co, S. C. Shim, C. S. Cho, T.-J. Kim, S. O. Kang, W.-S. Han, J. Ko and C.-K. Kim, *Organometallics*, 2005, **24**, 4824-4831.

25. F. Lorenzini, K. T. Hindle, S. J. Craythorne, A. R. Crozier, F. Marchetti, C. J. Martin, P. C. Marr and A. C. Marr, *Organometallics*, 2006, **25**, 3912-3919.
26. T. T. Co and T.-J. Kim, *Chem. Commun.*, 2006, 3537-3539.
27. R. Venkateswaran, M. S. Balakrishna and S. M. Mobin, *Eur. J. Inorg. Chem.*, 2007, **2007**, 1930-1938.
28. A. Buchard, E. Payet, A. Auffrant, X. Le Goff and P. Le Floch, *New J. Chem.*, 2010, **34**, 2943-2949.
29. A. Picot, H. Dyer, A. Buchard, A. Auffrant, L. Vendier, P. Le Floch and S. Sabo-Etienne, *Inorg. Chem.*, 2010, **49**, 1310-1312.
30. H. Dyer, A. Picot, L. Vendier, A. Auffrant, P. Le Floch and S. Sabo-Etienne, *Organometallics*, 2011, **30**, 1478-1486.
31. I. Bauer and H.-J. Knölker, *Chem. Rev.*, 2015, **115**, 3170-3387.
32. E. Balaraman, A. Nandakumar, G. Jaiswal and M. K. Sahoo, *Catal. Sci. Technol.*, 2017, **7**, 3177-3195.
33. D. Wei and C. Darcel, *Chem. Rev.*, 2019, **119**, 2550-2610.
34. A. Fürstner, *ACS Cent.*, 2016, **2**, 778-789.
35. K. S. Egorova and V. P. Ananikov, *Organometallics*, 2017, **36**, 4071-4090.
36. S. Wingerter, M. Pfeiffer, T. Stey, M. Bolboacá, W. Kiefer, V. Chandrasekhar and D. Stalke, *Organometallics*, 2001, **20**, 2730-2735.
37. P. B. Hitchcock, M. F. Lappert and Z.-X. Wang, *J. Organomet. Chem.*, 2008, **693**, 3767-3770.
38. T. Ogawa, T. Suzuki, N. M. Hein, F. S. Pick and M. D. Fryzuk, *Dalton Trans.*, 2015, **44**, 54-57.
39. T. Cantat, N. Mezailles, A. Auffrant and P. Le Floch, *Dalton Trans.*, 2008, 1957-1972.
40. T. K. Panda and P. W. Roesky, *Chem. Soc. Rev.*, 2009, **38**, 2782-2804.
41. M. Fustier-Boutignon, N. Nebra and N. Mézailles, *Chem. Rev.*, 2019, **119**, 8555-8700.
42. S. Al-Benna, M. J. Sarsfield, M. Thornton-Pett, D. L. Ormsby, P. J. Maddox, P. Bres and M. Bochmann, *J. Chem. Soc. Dalton Trans.*, 2000, 4247-4257.
43. K. Kreischer, J. Kipke, M. Bauerfeind and J. Sundermeyer, *Z. Anorg. und Allg. Chem.*, 2001, **627**, 1023-1028.
44. L. P. Spencer, R. Altwer, P. Wei, L. Gelmini, J. Gauld and D. W. Stephan, *Organometallics*, 2003, **22**, 3841-3854.
45. C. Winslow, H. B. Lee, M. J. Field, S. J. Teat and J. Rittle, *J. Am. Chem. Soc.*, 2021, **143**, 13686-13693.
46. N. M. Hein, F. S. Pick and M. D. Fryzuk, *Inorg. Chem.*, 2017, **56**, 14513-14523.
47. D. Adhikari, F. Basuli, H. Fan, J. C. Huffman, M. Pink and D. J. Mindiola, *Inorg. Chem.*, 2008, **47**, 4439-4441.
48. D. Buschhorn, M. Pink, H. Fan and K. G. Caulton, *Inorg. Chem.*, 2008, **47**, 5129-5135.
49. Y. Lee, N. P. Mankad and J. C. Peters, *Nat. Chem.*, 2010, **2**, 558-565.
50. D. L. M. Suess and J. C. Peters, *J. Am. Chem. Soc.*, 2013, **135**, 4938-4941.
51. J. Xiao and L. Deng, *Dalton Trans.*, 2013, **42**, 5607-5610.
52. D. Taher, J. R. Wilson, G. Ritch, M. Zeller and N. K. Szymczak, *Chem. Commun.*, 2021, **57**, 5718-5721.
53. A. Buchard, H. Heuclin, A. Auffrant, X. F. Le Goff and P. Le Floch, *Dalton Trans.*, 2009, 1659-1667.
54. E. Oheix, C. Herrero, J. Moutet, J. N. Rebilly, M. Cordier, R. Guillot, S. Bourcier, F. Banse, K. Sénéchal-David and A. Auffrant, *Chem. Eur. J.*, 2020, **26**, 13634-13643.
55. T. Cheisson and A. Auffrant, *Dalton Trans.*, 2016, **45**, 2069-2078.
56. T. Cheisson, L. Mazaud and A. Auffrant, *Dalton Trans.*, 2018, **47**, 14521-14530.
57. E. M. Schubert, *J. Chem. Educ.*, 1992, **69**, 62.
58. L. Yang, D. R. Powell and R. P. Houser, *Dalton Trans.*, 2007, 955-964.
59. R. G. Pearson, *J. Am. Chem. Soc.*, 1963, **85**, 3533-3539.
60. J. Zhang, M. Gandelman, D. Herrman, G. Leitus, L. J. W. Shimon, Y. Ben-David and D. Milstein, *Inorganica Chim. Acta*, 2006, **359**, 1955-1960.
61. A. W. Addison, T. N. Rao, J. Reedijk, J. van Rijn and G. C. Verschoor, *J. Chem. Soc. Dalton Trans.*, 1984, 1349-1356.
62. D. H. Nguyen, D. Merel, N. Merle, X. Trivelli, F. Capet and R. M. Gauvin, *Dalton Trans.*, 2021, **50**, 10067-10081.
63. N. E. Smith, W. H. Bernskoetter, N. Hazari and B. Q. Mercado, *Organometallics*, 2017, **36**, 3995-4004.
64. R. Langer, G. Leitus, Y. Ben-David and D. Milstein, *Angew. Chem. Int. Ed.*, 2011, **50**, 2120-2124.
65. T. Takeshita and Y. Nakajima, *Chem. Lett.*, 2019, **48**, 364-366.
66. T. Zell, R. Langer, M. A. Iron, L. Konstantinovski, L. J. W. Shimon, Y. Diskin-Posner, G. Leitus, E. Balaraman, Y. Ben-David and D. Milstein, *Inorg. Chem.*, 2013, **52**, 9636-9649.
67. N. I. Regenauer, H. Wadepohl and D.-A. Roşca, *Inorg. Chem.*, 2022, **61**, 7426-7435.
68. G. Jin, L. Vendier, Y. Coppel, S. Sabo-Etienne and S. Bontemps, *Dalton Trans.*, 2015, **44**, 7500-7505.
69. S. Takebayashi, M. A. Iron, M. Feller, O. Rivada-Wheelaghan, G. Leitus, Y. Diskin-Posner, L. J. W. Shimon, L. Avram, R. Carmieli, S. G. Wolf, I. Cohen-Ofri, R. A. Sanguramath, R. Shenhar, M. Eisen and D. Milstein, *Nat. Catal.*, 2022, **5**, 494-502.
70. S. Chakraborty, P. O. Lagaditis, M. Förster, E. A. Bielinski, N. Hazari, M. C. Holthausen, W. D. Jones and S. Schneider, *ACS Catal.*, 2014, **4**, 3994-4003.
71. Á. Raya-Barón, P. Oña-Burgos and I. Fernández, *ACS Catal.*, 2019, **9**, 5400-5417.
72. P. Bhattacharya, J. A. Krause and H. Guan, *Organometallics*, 2011, **30**, 4720-4729.
73. A. D. Smith, A. Saini, L. M. Singer, N. Phadke and M. Findlater, *Polyhedron*, 2016, **114**, 286-291.
74. A. M. Tondreau, E. Lobkovsky and P. J. Chirik, *Org. Lett.*, 2008, **10**, 2789-2792.
75. C. V. Thompson, H. D. Arman and Z. J. Tonzetich, *Organometallics*, 2022, **41**, 430-440.
76. G. Sheldrick, *Acta Crystallogr. A*, 2015, **71**, 3-8.
77. O. V. Dolomanov, L. J. Bourhis, R. J. Gildea, J. A. K. Howard and H. Puschmann, *J. Appl. Crystallogr.*, 2009, **42**, 339-341.
78. G. Sheldrick, *Acta Crystallogr. C*, 2015, **71**, 3-8.
79. L. J. Farrugia, Department of Chemistry, University of Glasgow, 2001.
80. N. G. Connelly and W. E. Geiger, *Chem. Rev.*, 1996, **96**, 877-910.
81. M. T. Reetz and E. Bohres, *Chem. Commun.*, 1998, 935-936.
82. K. T. K. Chan, L. P. Spencer, J. D. Masuda, J. S. J. McCahill, P. Wei and D. W. Stephan, *Organometallics*, 2004, **23**, 381-390.

83. K. D. Conroy, W. E. Piers and M. Parvez, *J. Organomet. Chem.*, 2008, **693**, 834-846.
84. C. J. Wallis, I. L. Kraft, J. N. Murphy, B. O. Patrick and P. Mehrkhodavandi, *Organometallics*, 2009, **28**, 3889-3895.
85. B. J. Ireland, C. A. Wheaton and P. G. Hayes, *Organometallics*, 2010, **29**, 1079-1084.
86. L.-C. Liang, F.-Y. Chen, M.-H. Huang, L.-C. Cheng, C.-W. Li and H. M. Lee, *Dalton Trans.*, 2010, **39**, 9941-9951.
87. T. Cheisson and A. Auffrant, *Dalton Trans.*, 2014, **43**, 13399-13409.
88. S. Ramírez-Rave, F. Estudiante-Negrete, R. A. Toscano, S. Hernández-Ortega, D. Morales-Morales and J.-M. Grévy, *J. Organomet. Chem.*, 2014, **749**, 287-295.
89. T. Cheisson, A. Auffrant and G. Nocton, *Organometallics*, 2015, **34**, 5470-5478.
90. S. Ramírez-Rave, M. T. Ramírez-Apan, H. Tlahuext, D. Morales-Morales, R. A. Toscano and J.-M. Grévy, *J. Organomet. Chem.*, 2016, **814**, 16-24.
91. L. Mazaud, M. Tricoire, S. Bourcier, M. Cordier, V. Gandon and A. Auffrant, *ORGANOMETALLICS*, 2020, **39**, 719-728.
92. A. T. Normand, R. Malacea-Kabbara, R. Lapenta, A. Dajnak, P. Richard, H. Cattey, A. Bolley, A. Grassi, S. Milione, A. Auffrant, S. Dagorne and P. Le Gendre, *Dalton Trans.*, 2020, **49**, 6989-7004.
1
2